Du, Xinming; Tan, Elaine S.; Elhan-Kayalar, Yesim; Sawada, Yasuyuki

Working Paper

Economic impact of COVID-19 containment policies: Evidence based on novel surface heat data from the People's Republic of China

ADB Economics Working Paper Series, No. 673

Provided in Cooperation with:
Asian Development Bank (ADB), Manila

Suggested Citation: Du, Xinming; Tan, Elaine S.; Elhan-Kayalar, Yesim; Sawada, Yasuyuki (2022) : Economic impact of COVID-19 containment policies: Evidence based on novel surface heat data from the People's Republic of China, ADB Economics Working Paper Series, No. 673, Asian Development Bank (ADB), Manila, https://doi.org/10.22617/WPS220243-2

ECONOMIC IMPACT OF COVID-19 CONTAINMENT POLICIES

EVIDENCE BASED ON NOVEL SURFACE HEAT DATA FROM THE PEOPLE'S REPUBLIC OF CHINA

Xinming Du, Elaine S. Tan, Yesim Elhan-Kayalar, and Yasuyuki Sawada

NO. 673

October 2022

ADB ECONOMICS WORKING PAPER SERIES

ASIAN DEVELOPMENT BANK

ADB

ADB Economics Working Paper Series

Economic Impact of COVID-19 Containment Policies: Evidence Based on Novel Surface Heat Data from the People's Republic of China

Xinming Du, Elaine S. Tan, Yesim Elhan-Kayalar, and Yasuyuki Sawada

No. 673 | October 2022

Xinming Du (xd2197@columbia.edu) is a PhD student at the Columbia University. Elaine S. Tan (estan@adb.org) is an advisor and head of the Statistics and Data Innovation Unit, Economic Research and Regional Cooperation Department, Asian Development Bank (ADB). Yesim Elhan-Kayalar (yelhan@adb.org) is an advisor at the Office of the Chief Economist, ADB. Yasuyuki Sawada (sawada@e.u-tokyo.ac.jp), former ADB chief economist, is currently professor of economics at the University of Tokyo.

The authors would like to thank Jisoo Hwang, Bryant Kim, and participants of the ERCD Seminar at ADB and 2021 Asia Impact Evaluation Conference for their constructive comments.

ASIAN DEVELOPMENT BANK

6 ADB Avenue, Mandaluyong City, 1550 Metro Manila, Philippines
Tel +63 2 8632 4444; Fax +63 2 8636 2444
www.adb.org

ISSN 2313-6537 (print), 2313-6545 (electronic)
Publication Stock No. WPS220243-2
DOI: http://dx.doi.org/10.22617/WPS220243-2

Notes:
In this publication, "CNY" refers to yuan and "$" refers to United States dollars.
ADB recognizes "China" as the People's Republic of China and "Korea" as the Republic of Korea.

CONTENTS

TABLES AND FIGURES

TABLES

FIGURES

ABSTRACT

Since the outbreak of the coronavirus disease (COVID-19) pandemic, governments around the globe have undertaken multiple policies to control its spread. Yet, only a few studies estimated the cost of COVID-19-related stringency measures on economic output, which can be attributable to the time lag and low frequency of conventional economic data. To bridge this gap in the literature, this paper uses novel high-frequency and spatially granular surface urban heat island (SUHI) data from satellites to quantify the impact of COVID-19-related containment policies in the People's Republic of China, exploiting variations in such policies. Three empirical results emerge. First, we find stringency measures decrease urban heat island in locked cities only marginally, which is equivalent to 0.04–0.05 standard deviation or CNY22.2 billion ($3.6 billion) of economic output drop which is a 0.09% annual gross domestic product decline in 2020. Second, our results suggest that governments have been learning continuously to manage containment measures better. Third, the government's containment policies have generated both positive and negative spillover effects on unlocked cities in which the former effect has dominated the latter.

Keywords: COVID-19 pandemic, economic costs of containment measures, surface heat island (SUHI) data from satellites, PRC

JEL codes: A10, O20

I. INTRODUCTION

The sudden emergence of the coronavirus disease (COVID-19) turned out to be one of the most devastating disasters in modern human history. One year after the first case was recorded, COVID-19 had afflicted more than 80 million people globally, taken 1.8 million lives, and set back global output by more than 2 years (ADB 2021). While it affected 3.2% of the working-age population globally in 2020, it is worth reaffirming that the pandemic is a health disaster, not an economic crisis, by nature. While substantial loss of life has had effects on employment and output directly, we can safely say that its economic impacts arise more from the containment policies rather than the disease itself. Since there have been intensive discussions around the world on the seemingly unavoidable trade-offs between the health and the economy (Peroff and Podolak-Warren 1979, Lin and Meissner 2020), it would be imperative to capture the economic impacts of pandemic containment policies accurately so that governments can identify and adopt appropriate policy instruments to control the pandemic. Yet, the lack of high-frequency, granular data prevent researchers from undertaking such assessments closely. To the best of our knowledge, only a few studies empirically estimated the causal impact of COVID-19-related stringency measures on economic output.[1] Indeed, the most authoritative review on the economics literature on the COVID-19 pandemic in developing countries mentions that "[a]n important open question is the role that government lockdown policies played in driving these adverse outcomes" (Miguel and Mobarak 2021). In this paper, we bridge this critical lacunae in the existing literature by using novel and innovative data, i.e., surface urban heat island (SUHI) data from satellites, focusing on the People's Republic of China (PRC).

The PRC provides an almost ideal setting for our analysis in two respects: First, it is an earliest example of lockdown measures with intermittent implementation of localized and city-wide lockdowns, allowing for a longer period of observations since January 2020 compared to other countries; and second, it covers a number of provinces with differentiated levels and timings of lockdowns. We take advantage of these policy variations which enable us to empirically identify the causal impact of public health response on economic output. In addition, the compliance rate with stringency measures and other applicable government policies has been higher in the PRC than in other countries,[2] which helps us to estimate the impact precisely. The high compliance rate implies our

[1] Conventional data on economic outputs is not available given the lag in data compiling and publication. Several papers use individual case study or model simulation to answer this question (e.g., Gunay, Can, and Ocak 2020; Havrlant, Darandary, and Muhsen 2021; and Shimul et al. 2021) without design-based empirical evidence. The closest work to this paper is by Beyer et al. (2020), which quantifies the impact of differential containment policies implemented by the Government of India during the COVID-19 pandemic on aggregate economic activity, using monthly nighttime lights as a proxy. Unlike their paper exploiting monthly variation from March 2020 to July 2020, we are able to capture daily changes in our economic outcome variable for a period from January 2016 and December 2020. Our data allows us to investigate time-changing nature of containment policy effectiveness explicitly. Also, by comparing nighttime lights data with our data explicitly, we can address potential bias arising from data on nighttime economic activities.

[2] The PRC tends to have high compliance rates on COVID-19 stringency for two reasons. First, culture norms affect compliance rates. Gelfand, Harrington, and Jackson (2017) and Bavel et al. (2020) have found some cultures, including the PRC, have strict social norms and punishments for noncompliance, and people in these cultures tend to follow government regulations in general. In the context of COVID-19, experimental evidence shows people in the PRC are willing to serve the collective goal of containing the COVID-19 (Dong et al. 2021). Second, from observed evidence, the PRC government adopts enforcement mechanisms like strict quarantines, quick response or QR codes, health risk ranking, and detailed contact tracing to control confirmed or potential cases. We confirm our compliance rate arguments in our mobility results: human movement largely decreases in both locked and unlocked cities when any PRC city is under lockdown.

estimated complier-average causal effect is similar to the average treatment effect without concerns of complier characteristics.[3]

To preview, there are three findings that emerged from our empirical analysis. First, we find COVID-19 stringency decreases economic output, measured by SUHI. Specifically, the locked cities experience 0.1°C lower SUHI because of lockdown relative to the unlocked cities, equivalent to 0.04–0.05 standard deviation of economic output drop. It is important to note that in the PRC, urban areas tend to have lower surface temperatures than rural areas, given that some industrial zones (that contribute to surface heat) are located away from cities, in more rural areas. For instance, 24.5% of coal power plants in the PRC are located in rural areas. These activities generate heat and result in hot rural areas. However, we note that regardless of the starting temperatures in urban areas, a decrease in surface heat during the lockdown period. Second, examining heterogeneous economic impacts because of the three differentiated levels of lockdown, i.e., complete lockdown, partial lockdown, and placement of checkpoints and quarantine zones, we find the most pronounced effects in completely locked cities, while lower effects in partially locked cities and cities with checkpoints. Third, we find both negative and positive spillover effects of the containment policies—mobility levels decreased in both locked and unlocked cities, despite SUHI increased in unlocked cities, suggesting that the positive spillover effects dominated the negative ones. Finally, we find that the negative economic impact of lockdown declined over time. This implies that governments have been learning continuously to manage containment measures better. We may also conclude there would have been negligible contribution of human movement to the PRC's SUHI, and a potentially substantial contribution of energy and industrial use.

We believe that our study contributes to existing studies in two aspects. First, we provide more accurate and frequent impact assessments of COVID-19 in the PRC by constructing a comprehensive and granular stringency measure of control policies for Chinese cities. While we are not the first to study COVID-19 stringency in the PRC, most existing papers use an indirect or less-precise measure as their treatment, including the number of cases in each city or the nationwide policy (Agarwal et al. 2020; Chen, Qian, and Wen 2021; Chen, Cheng, et al. 2020; Fang, Wang, and Yang 2020; Min, Xiang, and Zhang 2020; Ruan, Cai, and Jin 2021). In addition, a small number of studies use local stringency policies as treatment, but most of them stop before April 2020, focusing only on the first wave of COVID-19 outbreak (Chen, Li, et al. 2020; Fang, Wang, and Yang 2020; Kim and Zhao 2020; Zhang, Luo, and Zhu 2021). In contrast, we use the direct measure at the local level to construct our local stringency "treatment" variables. We also estimate impacts of the policies for the whole year 2020, covering not only the first wave in early 2020 but also during later outbreaks. The year-long study period provides a full picture of COVID-19 stringency impacts, allowing us to examine overtime changes of containment policy effectiveness. Besides, given the time period observed, our study is not affected by vaccinations which were rolled out extensively from February 2021 in the PRC. As vaccination may moderate the effect of COVID stringency and generate a downward bias, our study focusing on 2020 serves as a clean estimate of containment measures without the confounding effect of vaccinations.

[3] According to Angrist and Pischke (2009), we could only capture the causal effect of treatment on compliers, i.e., local average treatment effects, given partial compliance. Estimated effects are not generalizable to the entire population if the instrument induces a specific type of subpopulation. In contrast, we are able to capture the average treatment effect if the entire population follow policy instruments, like the case of the PRC.

Second, we measure changes in economic activities from satellite-based outcomes with high spatial resolution and temporal frequency. While SUHI has been studied in physical science fields on urban expansion, industrial relocation, and general human activities (Zhou et al. 2014, Li et al. 2017, Zhang et al. 2017, Wang et al. 2018, Alqasemi et al. 2021), to the best of our knowledge, this is one of the first studies in economics to employ SUHI to understand socioeconomic changes or to evaluate policies, especially in the context of the pandemic.

The remainder of this paper is organized as follows. Section II provides background on surface urban heat island. Section III describes the data for empirical analysis. Section IV discusses our empirical setting. Sections V and VI report the empirical results, mechanism discussion, and robustness tests. Section VII concludes.

II. SURFACE URBAN HEAT ISLAND

A. Definition and Cause

SUHI refers to the phenomenon that the surface of urban areas is significantly warmer than that in its surrounding rural areas. This phenomenon is commonly observed in large cities worldwide (Zhou, Rybski, and Kropp 2017) and is of great importance in sustainable city design. In the short run, the elevated temperature has adverse effects on human health and well-being, especially during heat waves. In the long run, local warming caused by higher heat discharge exacerbates global warming and could double the economic losses in the future.

Generally speaking, surface urban heat island is caused by several factors. The first is the albedo and infrastructure effect. Human-made materials used in urban areas such as asphalt pavements or metal roofing tend to reflect less solar energy and absorb more heat. Second, urban geometry also increases temperature. The space between buildings in the city is generally small, and this narrow space can restrict natural wind flows, slowing the heat release. Third, urban areas have fewer trees, vegetation, and water bodies. While these natural landscapes tend to cool the air, urban areas do not have them sufficiently by nature. Fourth, human activities can discharge heat. Vehicles, air conditioning, and industrial production facilities all emit heat to the urban environment. Therefore, surface temperature is generally higher in urban areas than that in rural areas, where the temperature is positively correlated with the level of anthropogenic activities. In the short run, daily variations in SUHI are most likely to be driven by contemporaneous human activity rather than the former three nonhuman factors which change overtime only slowly. Hence, changes in SUHI can be potentially considered as a real-time indicator of economic activity. All these factors result in SUHI, and we are not able to differentiate one factor from others.

B. Measures and Existing Studies

Measures of SUHI come from satellite thermal data. Imageries from Landsat were first applied to study SUHI in 1990 (Carnahan and Larson 1990). It has a high spatial resolution (60 m–120 m) but a lower time frequency (every 16 days) (Zhou et al. 2019). Besides, the Moderate Resolution Imaging Spectroradiometer (MODIS) Land Surface Temperature product is another important data source for SUHI research. It has a medium spatial resolution (1 km), and, more importantly, a high time

frequency (daily). Some other satellite sensors also provide thermal bands but are less frequently used in SUHI studies.[4]

The most widely used measure of SUHI is the difference in surface temperature between urban and surrounding areas. For example, Zhou et al. (2014) analyze the spatial variation in SUHI intensity and nightlight for 32 major cities in the PRC, finding a positive correlation between nightlight luminosity level and SUHI intensity. SUHI intensity is higher in southeastern and northern PRC where economic activities are higher. They also show SUHI intensity is more striking in summer than in winter during the day and the opposite during the night for most cities.[5] Using data for the United States, Li et al. (2017) report a nonlinear relationship between urban area size and SUHI. Doubling urban size could increase SUHI by 0.7°C. Similar to our study, Alqasemi et al. (2021) examine SUHI intensity change during COVID-19 lockdown in the United Arab Emirates. They use the blanket lockdown information combined with SUHI intensity data to perform a before-and-after comparison between 2020 and 2019. They find lockdown is associated with a lower SUHI intensity by 19.2%.

III. DATA

In this study, we employ SUHI intensity data in each city together with detailed information on COVID-19 response stringency data.

A. COVID-19 Response Stringency

We construct our "treatment" variable—COVID-19 response stringency at the city-day level—by collecting information about local policies from government announcements and news media. After gathering all the stringency actions, we generate five indicators, i.e., three levels of lockdown indicators as well as two indicators for school closure and workplace closure.[6] We extend Fang, Wang, and Yang (2020) and classify lockdown into three complete and mutually exclusive levels: complete lockdown, partial lockdown, and placement of checkpoints and quarantine zones. The classification is based on two objective information, i.e., move-out ban and public transportation cancellation.[7]

---

[4] The review by Zhou et al. (2019) shows the proportion of the existing studies using different sensors. Landsat takes 53% and MODIS takes 25% of the total SUHI studies they reviewed.

[5] We use SUHI rather than nightlight as a proxy for economic output in this study as SUHI has daily frequency while nightlight is monthly. As the PRC's lockdown usually takes place promptly and lasts for 2 weeks, we are interested in daily variation of economic activities.

[6] Note that we refrain from using data on testing intensity, face mask wearing, or social distancing as elements for our stringency indicator. On the one hand, these policies are not formally regulated by the government, and thus do not necessarily provide useful exogenous policy variations in identifying policy effects. On the other, these indicators may have been driven by lockdown and are more likely to be outcome variables, rather than policy variables.
We do not use school or workplace closing and only focus on lockdown indicators in the empirical estimation. Lockdown serves as a general, comprehensive stringency control including school closing and workplace closing measures. The latter two are correlated with lockdowns. Also, we have less precise information on school and workplace closing from government documents and media, while clear and well-enforced dates of lockdown start and end.

[7] There is no official classification of lockdown levels by the Government of the PRC. Though central governments flag high-risk and medium-risk areas in some cities, this scheme started in April 2020 and could not cover the first outbreak in early 2020.

Among these three types of lockdowns, complete lockdown is the most stringent control. Residents are not allowed to leave the city. For within-city movement, both public transport and private transport are forbidden. All residential housing estates are under lockdown and residents are allowed to leave their apartments only with limited quota for essential activities. Partial lockdown is the second most stringent one. Residents are allowed to leave the city. Public transport has been temporarily shut down, but private transport is allowed. The least stringent lockdown is checkpoints and quarantine zones. This indicator takes a value of one if there is at least one quarantine zone (which could be as small as a housing estate) in the city on that day.

Figure 1 visualizes our stringency measure, displaying the number of cities with some lockdown on each day. In Panel A, the blue line is the number of cities with any level of lockdown. While the number of locked cities reached more than 100 in February 2020, it decreased to zero in April 2020. We have another lockdown peak in July and August, including Beijing and Xinjiang Uygur Autonomous Region (XUAR) lockdowns. Shaded areas in Panel A indicate lockdown-free time—totaling 63 days in 2020 without any city under lockdown in the PRC. In Panel B, the number of cities with complete and partial lockdowns are shown, respectively, in red and green lines (left Y-axis). Blue dash lines indicate the least stringent lockdown (right Y-axis). Complete lockdown peaked twice in 2020—in February and March and in summer.

B. Surface Heat

We employ MODIS daytime land surface heat product to construct SUHI variable. MODIS is the key instrument aboard satellite Terra launched in 1999. Terra views the entire Earth's surface every day at 10:30 am local solar time in 36 spectral bands ranging in wavelengths 0.44 μm–14.4 μm. The land surface temperature product is developed based on three thermal infrared bands. Its spatial resolution is 1 km and its time frequency is 1 day. We use daytime land surface temperature in our main result and nighttime land surface temperature in the robustness check.

To process heat data from pixel–day level to city–day level, we need to calculate each city's surface temperature at the urban–day and rural–day level. Two base maps are used for data processing. First, we use a prefecture-level city base map for the PRC from the Center for Geographic Analysis at Harvard University.[8] There are 339 cities in total, and each city refers to one polygon. We project cities on the satellite product, and each city covers some 1 km pixels. We calculate the average values of the covered pixels as surface temperature for that city on that day.

We use urban boundary map from the global artificial impervious area (GAIA) (Li et al. 2020),[9] and conduct a similar projection for each urban area. Then we calculate the weighted average of urban temperature and rural temperature for each city (weighted by the number of covered pixels). We use the simple difference between urban heat and rural heat as our measure for SUHI intensity.

[8] Center for Geographic Analysis. China GIS Data. https://gis2.harvard.edu/resources/data/china-gis-data (accessed 31 January 2021).

[9] Department of Earth System Science, Tsinghua University. Global Land Cover. http://data.ess.tsinghua.edu.cn/ (accessed 31 March 2021).

C. Mobility

We use mobility indexes from Baidu, which is the dominant search engine in the PRC as Google does not operate in the PRC since 2010.[10] Baidu Migration uses Baidu Map location-based service to estimate mobility index. Mobility indexes are based on Baidu Map users' location change, no matter what type of transport. In this study, we use three mobility indexes: within-city mobility index, move-in index, and move-out index. They are comparable across cities and time. To construct our outcome variables, we aggregate these indexes into the city–day level index. Because of limitation of data availability, we only use the index that covers 1 January 2020–3 May 2020.

D. Economic Outputs

We also extract and use commonly used economic output variables from CEIC Global Database to validate our SUHI measures. We use gross domestic product (GDP) at the city–quarter level, household expenditure per capita at the city–quarter level, and government revenue at the city–month level for validation tests.

IV. EMPIRICAL STRATEGY

To evaluate the impact of COVID-19-related stringency measures on economic outputs captured by SUHI, we exploit variations in stringency measures across cities and time for 2016–2020. Specifically, we use the standard difference-in-differences design:

$$Y_{it} = \beta_0 + \beta_1 LockAnyCity_t + \beta_2 Locked_{it} + \theta_t + \gamma_i + \varepsilon_{it}, \quad (1)$$

where Y_{it} is outcome variable, SUHI intensity, of city i on date t. The use of SUHI intensity has been common in the existing studies such as Zhou et al. (2014) because it can eliminate the geographical differences in climate conditions in different cities and short-term weather fluctuations. We also analyze mobility indexes as an outcome Y in the mechanism section. On the right-hand side of equation (1), $LockAnyCity_t$ is an indicator variable which takes one if any city in the PRC is being locked on day t; and zero otherwise. Note that this variable takes the same value for all Chinese cities and for any lockdown of the three levels. The term $Locked_{it}$ captures city i being locked on day t by taking one for a locked city on its locked day, and zero otherwise. It also captures any lockdown of the three levels.

In terms of other controls, γ_i includes city fixed effects. θ_t captures time fixed effects including day-of-week, month, and year. β_2 is the coefficient of chief interest. It shows the impact of lockdown on locked cities relative to unlocked cities. If lockdown reduces economic activities, we expect β_2 to be negative. Coefficient β_1 measures the national level impact of any city's lockdown on all Chinese cities through different channels such as the ones through supply–chain networks as well as changes in sentiments of consumers and producers.

[10] Baidu. Baidu Migration. https://qianxi.baidu.com/ (accessed January 25, 2021).

We further separate three levels of lockdown to test the heterogeneity across stringency levels. The specification is:

$$Y_{it} = \beta_0 + \lambda_1 LockAnyCity1_t + \lambda_2 LockAnyCity2_t + \lambda_3 LockAnyCity3_t + \theta_1 Locked1_{it} + \theta_2 Locked2_{it} + \theta_3 Locked3_{it} + \theta_t + \gamma_i + \varepsilon_{it} \quad (2)$$

where *LockAnyCity*1_t, *LockAnyCity*2_t, and *LockAnyCity*3_t, respectively, indicate any Chinese city that is under complete lockdown, partial lockdown, and have checkpoints or quarantine zones on day t. Similarly, *Locked*1_{it}, *Locked*2_{it}, and *Locked*3_{it} denote that city *i* is under each level of lockdown.

Since we use a complete and exclusive lockdown classification, by definition, we have: *Locked*1_{it} + *Locked*2_{it} + *Locked*3_{it} = *Locked*$_{it}$, and *LockAnyCity*1_t + *LockAnyCity*2_t + *LockAnyCity*3_t = *LockAnyCity*$_t$. When there are two cities under different levels of lockdown, we use the most stringent control among all the cities on day *t*.

Finally, we simplify the empirical strategy of Miguel and Kremerb (2004) to test the spillover effect of COVID-19 stringency on adjacent cities and non-adjacent cities in the same province:

$$Y_{it} = \alpha_0 + \alpha_1 LockAnyCity_t + \alpha_2 Locked_{it} + \alpha_3 LockAnyCity_t \times Adjacent_{it} + \alpha_4 LockAnyCity_t \times NonAdjacent_{it} \times SameProvince_{it} + \theta_t + \gamma_i + \varepsilon_{it}, \quad (3)$$

where *Adjacent*$_{it}$ takes one if city *i* shares border with a city under lockdown on day *t*; *NonAdjacent*$_{it}$ takes one if city *i* does not share border with a city under lockdown on day *t*; and *SameProvince*$_{it}$ takes one if a city under lockdown on day *t* is in the same province. If there is a negative spillover effect across city border, we expect that the estimated α_3 is negative.

Since cities and residents in the same province are connected with each other through supply chain networks and other channels, we test whether non-neighbor cities in the same province are also affected differently, compared with cities in lockdown-free provinces. To do so, we add the triple interaction term, *LockAnyCity*$_t$×*NonAdjacent*$_{it}$×*SameProvince*$_{it}$, which takes one if city *i* is in the same province as a lockdown epicenter on day *t*; and zero otherwise. Considering negative spillover effects within the same province, the estimated coefficient α_4 is hypothesized to be negative.

V. RESULTS

A. Correlation Between Surface Urban Heat Island and Economic Output

To validate our measure, we first test the correlation between surface urban heat island and conventional economic output variables. Specifically, we use GDP at the city–quarter level, household expenditure per capita at the city–quarter level, and government revenue at the city–month level. Since data covers the period from 2016 to 2020, we are able to test the correlation both before and during the pandemic. Table 1 displays empirical results from regressing SUHI intensity on each of the economic variables, showing overall positive and fairly significant coefficients. These results indicate our SUHI intensity measure is a reasonable proxy of the economic output measures. Particularly, the

correlation is still positive and statistically significant for GDP even if we include time-varying (city–month) fixed effects. SUHI seems to capture granular intra-month information about economic activities within each city which cannot be captured by GDP.

We also check the relationship between SUHI intensity and mobility indexes, though we have a short time period for this analysis. As we can see from Table 2, SUHI intensity captures both the time variation and the spatial variation of the within-city mobility index quite well. As discussed in Section II, vehicle use and transportation contribute to the urban heat island. Despite the strong correlation, we still cannot conclude whether urban heat island in the PRC is driven by human mobility or other activities, such as energy and industrial use that are closely correlated with mobility patterns. In contrast, SUHI intensity correlates weakly or negatively with across-city mobility indexes, a finding that possibly reflects human responses to temperature—we expect lower heat generation in urban areas when residents move out of the city; and also, rural areas tend to be hotter with higher level of move-in population.

Apart from these correlation tests, we show the time series data of SUHI intensity in Figure 2.[11] Taking the whole country together, SUHI intensity shows a strong seasonality, with higher values in winter and lower values in summer.[12] SUHI intensity ranges from -1°C to 0°C, and there is no obvious outlier in the 5-year graph. When we zoom in to the areas of top interest, Hubei, Beijing, and Tianjin show different local seasonalities. Compared with Beijing and Hubei, SUHI intensity values in XUAR have more significant deviations over time, probably because of XUAR's fluctuating socioeconomic activities over time. Focusing on the lockdown periods, SUHI intensity values slightly decreased during the lockdown in Hubei and XUAR, while the pattern is less evident for Beijing.

B. Effects of COVID-19 Response Stringency on Surface Urban Heat Island

We plot the same-day difference of SUHI intensity between the treated year 2020 and earlier 2 years' average in Figure 3. In Panel A, red dots are weighted average SUHI intensity for all treated cities under lockdown on each day, with weights equal to urbanization rates. Blue dots are weighted average SUHI intensity for all control cities and treated cities not under lockdown. In panels B–D, red lines are the lockdown or "treated" regions, including Hubei, Beijing, and XUAR, and blue lines are their local neighbor regions without lockdown.[13] The first and second vertical gray lines in each chart are, respectively, local lockdown's start and end dates. In Panel B, Hubei shows a different trend with its neighbor before the lockdown started, and still behaved differently until the lockdown ended. After that, Hubei and its neighbor show parallel trends in the rest of the year. The pre-trend is probably because of the internal information of COVID-19 before the official lockdown started. Unlike later outbreaks with fast policy responses, the first case in Hubei occurred in late 2019, about 1 month before the lockdown started on 23 January 2020. Thus, people may already have behavioral responses before the stringency policy. After the lockdown ended in April, life got back to normal, and we see very similar curves for Hubei and Hunan.

---

[11] We use urbanization rate to weight cities and calculate the average SUHI for the whole PRC. In Table 2.1 and Figure 2.1, we show a positive cross-sectional correlation between urbanization rate and SUHI at the city level.

[12] We expect a positive SUHI if urban areas are generally hotter than rural areas. However, the average value of SUHI in the PRC is -0.2°C. One potential reason is the relocation of industrial facilities in rural areas when more people move to the urban. We check the spatial distribution of 2,029 Chinese coal-fired power plants using data from CoalSwarm (https://endcoal.org/global-coal-plant-tracker/), and 498 (24.5%) of them are located out of the urban boundary. Besides, our negative SUHI taking all Chinese cities together is consistent with existing papers (Zhou et al. 2014, Zhou et al. 2015, Li and Zhou 2019, Niu et al. 2020) that also document negative SUHI values.

[13] We use geographic neighbors of treated regions as control regions. While each treated region has multiple unlocked neighbors, they show similar SUHI patterns and the choice of control regions does not change the figure.

In Panel C, Beijing got lockdown in June and reopened in July. Beijing and its neighbor Shanxi behaved very similarly in the pre-period, and Beijing's heat island decreased during its lockdown. After that, Beijing had a strong rebound effect, probably because of an accelerated economic recovery after the COVID-19 is controlled. In Panel D, we see similar patterns for XUAR as that for Beijing and its neighbor during the lockdown. There is no rebound effect in and after September in XUAR.

Why did Beijing experience a unique rebound pattern? One potential reason is Beijing's different economic structure. Beijing has a higher concentration of the services sector. Compared with manufacturing and other sectors, it will be straightforward for the services sector to be reopened after governments provide some consumption incentives. Beijing also has a larger population, and recovery can be easier when there are more consumers and more labor services. Further, Beijing's lockdown involved isolated checkpoints, compared with the other two regions with a broad, large-scale lockdown. The isolated checkpoints mean a less-stringent treatment and an easier recovery.

Table 3 shows estimation results based on equation (1). Taking three levels of lockdown together, lockdown decreases locked cities' heat island by 0.04–0.05 standard deviation, while slightly increases unlocked cities' heat island by 0.01–0.02 standard deviation.[14] The decrease is consistent with intuition. Lockdown reduces human mobility, economic production, and anthropogenic activities, resulting in overall lower heat generation. Based on the correlation test in Table 1, locked cities observe reductions in quarterly GDP, quarterly household expenditure per capita, and monthly government revenue, respectively, by CNY22.2 billion, CNY793 billion, and CNY5.33 billion. Unlike locked cities, those without stringency control have an increased SUHI intensity. Section IV discusses this finding and potential mechanisms.

C. Heterogeneity Across Stringency Levels, Over Time, and Spillover Effects

In further quantifying the impact of stringency measures, we separate three levels of lockdown by estimating equation (2). Table 4 shows that a complete lockdown has the largest negative effect on locked cities' heat island. Partial lockdown, checkpoints, and quarantine zones have slightly negative effects. As complete lockdown bans public and private transport, and partial lockdown bans public transport only, one possible reason behind this heterogeneity is the large role that private transport, such as cars, plays in generating urban heat. Another potential reason could be that public transport commuters do not switch in large numbers to private cars during partial lockdowns.

In Table 5, we assess the impact of stringency on adjacent cities and other cities in the same province, relative to other cities outside the province. The observed higher SUHI intensity in unlocked cities is mainly driven by non-adjacent cities within the same province, possibly because of production relocation channels. We will explore potential mechanisms for the estimated patterns in the following section.

Moreover, we test heterogeneous treatment effects over time in Table 6 and Table 7. When adding a linear time trend and an interaction term $Locked_{it} \times Days$, positive estimates on the interaction term indicate that the negative effects of lockdown on treatment are getting smaller over time. Specifically, lockdown on 1 February 2020 decreased locked cities' SUHI more than lockdown on 11 May 2020 (100 days later) by 0.1°C. Separately estimating treatment effects in each month in

[14] We find imprecise estimates on $Locked_{it}$ in column (2) when city–month FEs are added. City–month FEs may capture our treatment given a small number of years and the monthlong lockdown period in 2020. We focus on columns (1), (3), and (4) when interpreting our results.

2020 shows that the most severe economic loss because of lockdowns occurred in February, March, and September 2020. Estimates are getting larger over time, indicating gradually lower economic costs arising from the lockdown. This suggests a "learning-by-doing" effects of the governments in managing containment measures by better balancing public health benefits and economic costs in later COVID-19 waves.

VI. DISCUSSION ON MECHANISM

A. Effects of COVID-19 Response Stringency on Human Mobility

Why does lockdown reduce surface urban heat island in locked cities? While we are unable to disentangle the contribution of each sector to the observed lower level of SUHI intensity, anthropogenic activities such as energy use, industrial productions, and vehicle and human movement are more likely to be affected by the COVID-19 stringency, compared with human-induced land use change and other structural transformation that are less likely to vary in the short run. Using Baidu mobility data, we assess the impact of the COVID-19 stringency on human movement so that we can identify mechanisms behind the stringency and SUHI intensity nexus at least partly. We hypothesize that lockdown reduces human movement as an intermediate route, which in turn results in lower SUHI intensity.

With mobility indexes as outcome variables, Table 8 displays results from estimating the regression model of equation (1). Negative and precise estimates on $Locked_{it}$ confirm our basic hypothesis—lockdown drives down locked cities' within-city, move-in, and move-out mobility index by 2.26, 0.86, and 1.06 points, respectively, equivalent to 55%, 105%, and 135% relative to the mean. Results are robust even if we control for national and local seasonality [columns (1) and (2)], and are robust in the same-month and same-day comparison [columns (3) and (4)]. The model achieves the highest explanatory power (i.e. the largest R^2 value) in column (2), indicating that mobility pattern shows strong local seasonality.[15]

Estimated coefficients on $LockedAnyCity_t$ are also negative and significant consistently, which suggest unlocked cities also witness lower mobility patterns despite no stringency policies imposed. Specifically, their within-city, move-in, and move-out pattern drop, respectively, by 1.87, 0.50, and 0.52 points, namely 45.5%, 61.5%, and 62.8% relative to the mean. After removing the nationwide effect, locked cities experience a more considerable drop in across-city migration than intracity migration, as shown in the relatively larger estimates on $Locked_{it}$ in panels B and C.

If human movement drives the SUHI pattern, we would expect a positive estimate on $LockedAnyCity_t$ and a negative one on $Locked_{it}$. Empirically, effects on mobility are consistent with those on SUHI in cities that implemented lockdown measures, but not consistent with cities without lockdown measures. One explanation for this finding is that human movement is not a key driver for SUHI change in our main results. Although human movement contributes to SUHI, the increased SUHI in unlocked cities is likely to result from other anthropogenic activities like industrial facilities, air

[15] We do not test the heterogeneous mobility effects by lockdown levels because of the collinearity of complete and partial lockdown city–day during January 2020–April 2020.

conditioning, and energy use. Another interpretation is a possible shift in human behaviors. For cities not in lockdown, mobility nevertheless falls probably because of fear, so we capture a negative estimate on $LockedAnyCity_t$ in Table 8. SUHI, however, does not decline because of the other non-mobility sectors that also contribute to SUHI, so the estimate is positive in Table 3.

B. Other Potential Mechanisms

One potential reason behind the SUHI intensity decline because of lockdown is the production shift. With some cities under lockdown, production and supply chains tend to be moved to unlocked cities to ensure necessary supply and national development. If the supply chain network within the PRC is fairly resilient against disasters, it is not too costly to change production location from one branch to another. Accordingly, higher production activities in unlocked cities might have led to higher SUHI there.

Another potential mechanism might be the relaxation of environmental regulation during the pandemic. For each production unit, heat discharge in unlocked cities may be higher than in earlier years without COVID-19. Heat discharge is one dimension of green production and sustainability. Indeed, in March 2020, governments waived environmental impact assessment rules and removed requirements for on-site inspections to curb the economic damages caused by COVID-19.[16] Given a different policy priority on controlling COVID-19 and maintaining economic output, a lenient environmental regulation may increase heat discharge and result in a higher SUHI.

C. Robustness Checks

We also perform a series of robustness checks to validate our findings, including placebo tests, adding group-specific time trends, lunar calendar (to account for potential seasonal changes in overall mobility and SUHI), and nighttime heat island data.

1. Placebo Test

We conduct a falsification analysis to check for "placebo" effects on outcomes that are known to be unaffected by the treatment (e.g., outcomes measured before the treatment). In this case, we have used placebo treatment dates, which are from 1 year prior, and dropped the year 2020. Table 9 shows the estimation results in which we find no significant effects of placebo lockdown variables on locked cities' SUHI, validating our identification strategies of COVID-19 impacts.

2. Adding Group-Specific Time Trends

Human-to-human transmission accounts for a significant portion of COVID-19 cases, and larger cities with more population and higher mobility rates have higher risks of COVID-19 outbreaks. However, cities that were locked early and treated cities might have had inherently different experiences from unlocked cities. In this context, if larger cities have different SUHI trajectories over time, e.g., a slower growth rate, we may still observe a negative coefficient on the lockdown variable, $Locked_{it}$, even when lockdown has no effect on SUHI intensity.

[16] Muyu Xu and Brenda Goh. 2020. "China to modify environmental supervision of firms to boost post-coronavirus recovery." *Reuters*, March 10. https://www.reuters.com/article/us-health-coronavirus-china-environment-idINKBN20X0AG.

To address this potential endogeneity bias, we included group-specific linear time trends additionally and re-estimated our models. Findings summarized in Table 10 suggest our results remain qualitatively the same as the main findings reported in Table 3, leading us to conclude that unobserved time trends do not solely drive observed SUHI patterns.

3. Using Lunar Calendar

Given significant behavioral changes in consumer and producer behaviors in the PRC around the Chinese New Year, and resultant potential seasonality, we employ the lunar calendar to define and include our month and year fixed effects. The estimation results reported in Table 11 confirm that our findings are stable with this alternative calendar definition. The SUHI intensity still decreases in locked cities and increases in unlocked cities even after lunar patterns are controlled.

4. Nighttime Heat Island

Daytime heat island data capture human movement and industrial use, while nighttime temperature differences are mainly driven by nighttime energy use in public roads and residential sectors. As another robustness check, we use nighttime heat island data as an alternative to daytime SUHI and re-estimate equation (1). Estimation results are reported in Table 12, and show essentially same findings, i.e., negative effects on locked cities and positive effects on unlocked cities. Further, estimated magnitude of 0.02–0.04 standard deviation declines in surface temperature during nighttime, indicating that lockdown has larger impact on industrial sectors that operate in the daytime.

VII. CONCLUSION

Benefits of COVID-19 stringency measures on public health and pandemic containment have been discussed extensively. However, the cost of COVID-19 stringency measures on economic output is less known. The challenge in understanding this cost is mainly driven by the discrepancy between the speedy and variable nature of COVID-19 pandemic spread, governments' responses to the pandemic, and the low frequency of verified conventional economic data. In this study, we overcome this challenge by using daily urban heat island as a proxy for economic output.

First, we find urban heat island can capture economic activities and human mobility reasonably well. Second, while urban areas are cooler in PRC than the rural areas in general, we show COVID-19 lockdowns further decrease urban heat island in locked cities by 0.04–0.05 standard deviation. This connotes decreases in quarterly GDP (CNY22.2 billion), quarterly household expenditure per capita (CNY793 billion), and monthly government revenue (CNY5.33 billion). The decrease in SUHI is more pronounced under complete lockdown conditions, compared to cities under partial lockdown and checkpoints, which show similar effects albeit of a smaller magnitude. This variation is possibly attributable to operation of private vehicles, which are banned under complete lockdown but permitted to operate under partial lockdown.

Third, we show urban heat island increases in unlocked cities when other cities are under lockdown, even though mobility patterns decrease in both locked and unlocked cities. This inconsistency could be attributable to either the small contribution of human movement to the PRC's

SUHI intensity, or it could be a behavioral response whereby fear of infection causes a decline in mobility even in unlocked cities. We further propose two potential reasons behind the higher urban heat island in unlocked cities—the production shift from locked to unlocked cities and lenient environmental regulations that allow for increased production with high heat emissions in unlocked cities. A closer look at the mechanisms and transmission channels with more granular data could be useful in exploring this line of thought further in the future.

Finally, beyond the empirical analysis pertinent to specific cities in the PRC, our findings suggest three key areas for further attention of policymakers at large. First, mobility decreases in both locked cities and unlocked cities during the period when lockdown measures are implemented. This negative externality signals a need for post–COVID-19 pandemic economic recovery measures that target not only locked cities but also unlocked ones. Second, our approach can augment real-time tracking of compliance with mobility restrictions imposed during lockdown periods. Our methodology of using SUHI intensity data can be applied to other countries that lack high-frequency data on ground-based mobility. Response in SUHI can indicate the extent to which people follow public health policies and decrease their outdoor activities during lockdown periods. Third, our findings indicate that, to simultaneously address intensifying urban heat island phenomena and for green development going forward, government policies may need to put more focus on how different modes of transportation may impact SUHI levels in urban and peri-urban areas, and the effect of different types of industrial production (with varying environmental regulatory frameworks) on SUHI levels.

Figure 1: Visualization of COVID-19 Response Stringency in the People's Republic of China

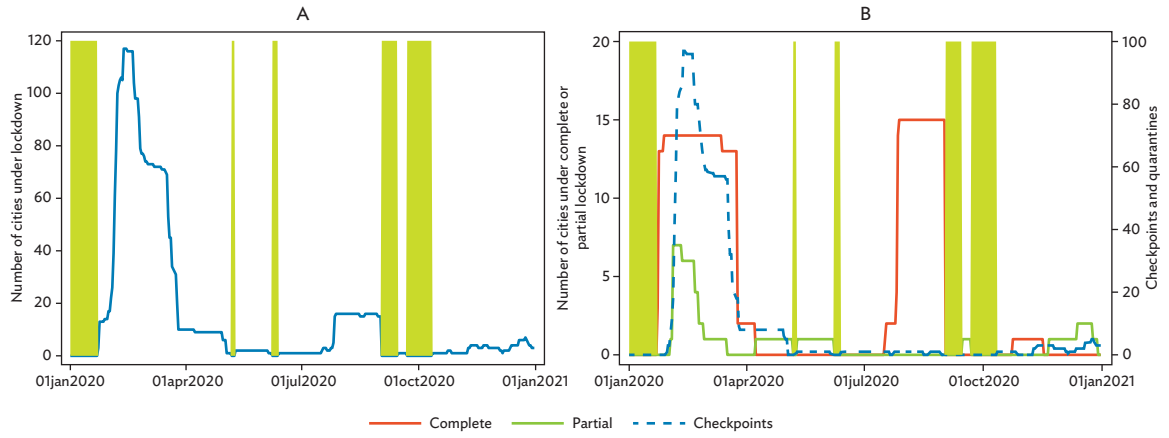

Note: Panel A: Number of cities with any level of lockdown. Panel B: Number of cities with each level of lockdown.
Source: Authors' calculations using self-constructed stringency panel described in Section III.A.

Figure 2: Time Series of Surface Urban Heat Island Intensity, 2016–2020

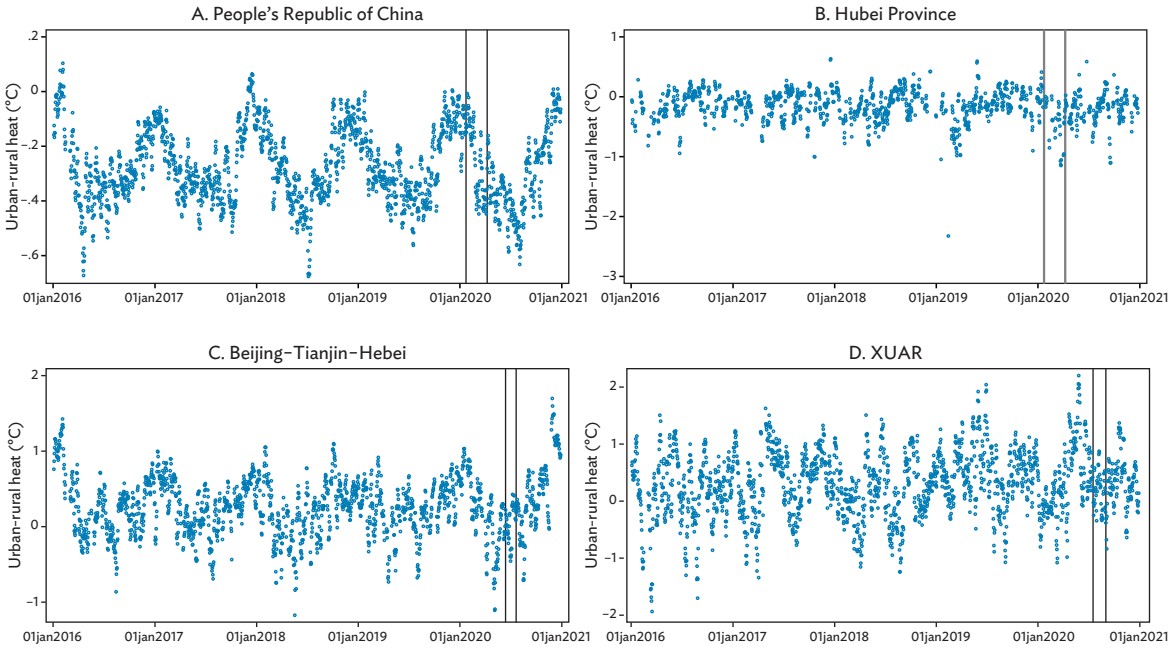

XUAR = Xinjiang Uygur Autonomous Region.

Notes: Figure 2 shows the simple difference between urban heat and rural heat on each day, following the well-used surface urban heat island (SUHI) intensity measure (e.g., Zhou 2014). Panel A: All Chinese cities weighted by urbanization rates. Panel B: SUHI series in Hubei province. Panel C: SUHI series in Beijing–Tianjin–Hebei region. Panel D: SUHI series in XUAR. Gray vertical lines are local lockdown start and end dates.

Source: Authors' calculations using SUHI data from MODIS, described in Section III.B.

.

Figure 2.1: Quadratic Fit of Urbanization Rate and Surface Urban Heat Island

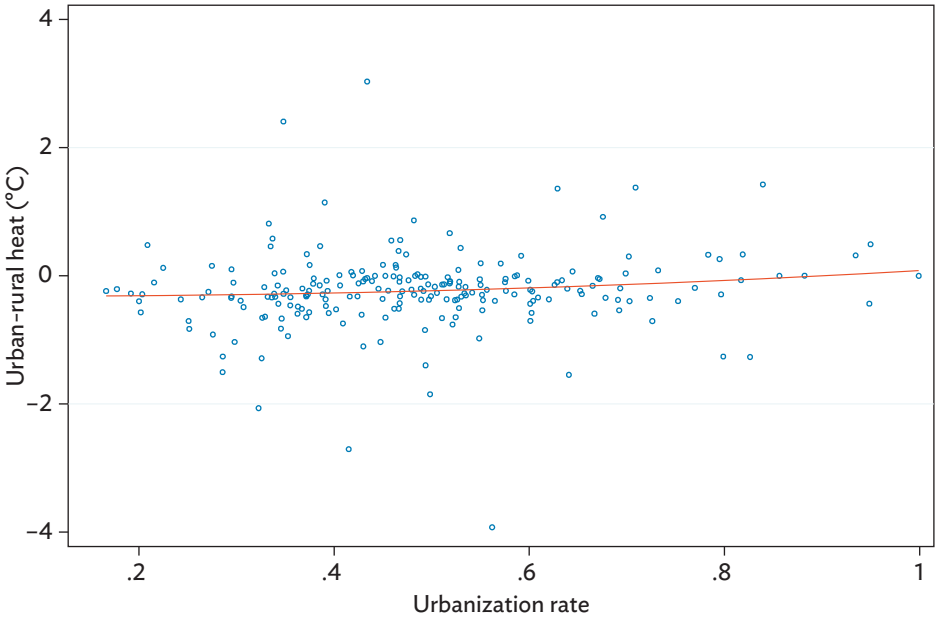

Note: The blue dots show raw urbanization rate and surface urban heat island (SUHI) values. The red line displays the quadratic fitted curve. The curve is close to linear, which suggests a positive correlation between urbanization rate and SUHI.

Source: Authors' calculations using SUHI data from MODIS and urbanization rate data from CEIC, described in Section III.B and III.D respectively.

Figure 3: Surface Urban Heat Island in Treated and Control Regions

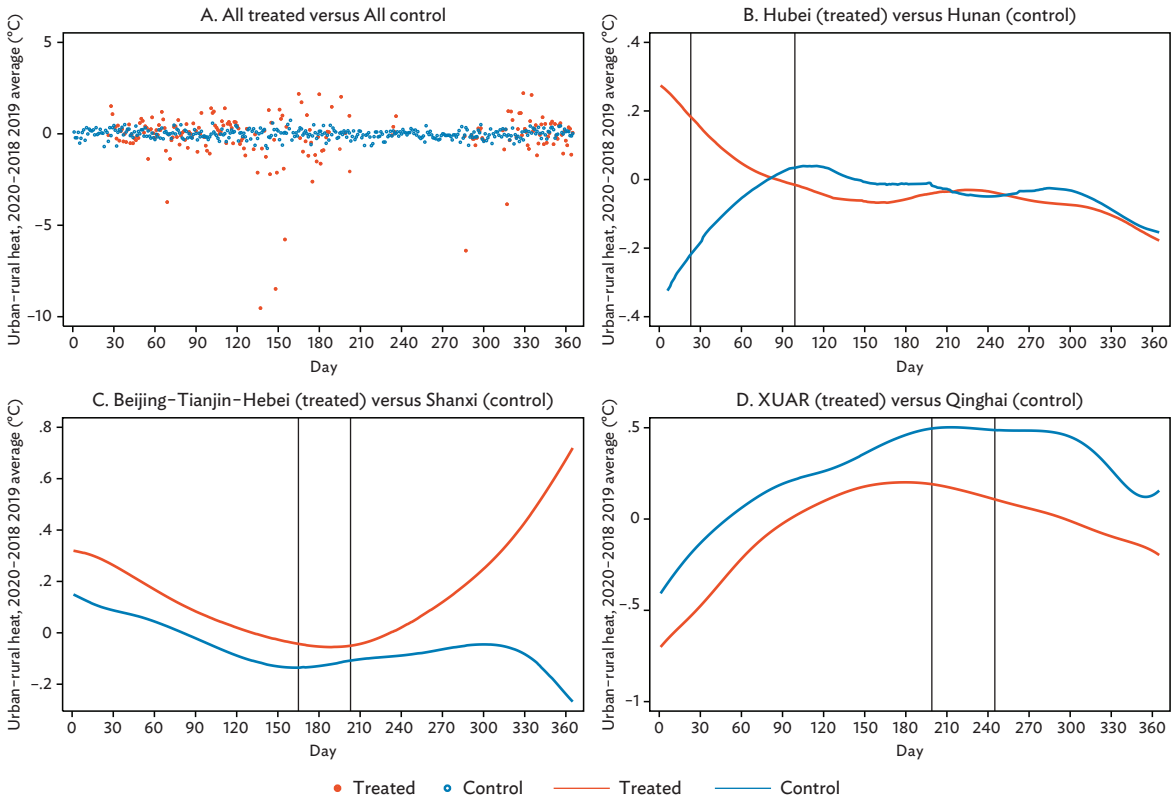

XUAR = Xinjiang Uygur Autonomous Region.

Note: Figure 3 displays same-day surface urban heat island (SUHI) intensity difference in the treated year 2020 and the average level in 2018–2019. Gray vertical lines are local lockdown start and end dates.

Source: Authors' calculations using SUHI data from MODIS, described in Section III.B.

Table 1: Correlation Between Surface Urban Heat Island Intensity and Economic Outputs

	Urban Heat Islands (°C)			
	Panel A: With Gross Domestic Product			
	(1)	(2)	(3)	(4)
GDP	4.470***	4.324***	0.819*	1.942***
(CNY trillion)	(0.910)	(0.898)	(0.450)	(0.744)
Observations	4,130	4,130	4,130	4,130
R-square	0.212	0.214	0.868	0.670
	Panel B: With Household Expenditure			
Expenditure	0.121***	0.121**	−0.013	0.036
(CNY'000)	(0.030)	(0.030)	(0.068)	(0.090)
Observations	367	367	367	367
R-square	0.201	0.211	0.871	0.765
	Panel C: With Government Revenue			
Government revenue	0.018***	0.018***	0.008**	0.005
(CNY billion)	(0.003)	(0.003)	(0.003)	(0.003)
Observations	1,1721	1,1721	1,1721	1,1721
R-square	0.160	0.160	0.836	0.703
City FEs	Y	Y		
Month FEs		Y		
Year FEs		Y	Y	
City–month (city–quarter) FEs			Y	
Year–month (year–quarter) FEs				Y

DOW = day of week, FE = fixed effect, GDP = gross domestic product.

Note: Standard errors in parentheses are clustered at the city level. In Panel A, we have 4,635 GDP values at the city-quarter level, and 4,130 of them have non-missing heat island data. In Panel B, there are only 367 observations at the city–quarter level for 2016–2020, mainly because of limited availability of CEIC expenditure data for cities with heat island data for this period. *** = p < 0.01, ** = p < 0.05, * = p < 0.1.

Source: Authors' calculations using surface urban heat island data from MODIS and economic data from CEIC, described in Sections III.B and III.D respectively.

Table 2: Correlation of Surface Urban Heat Island and Mobility Indexes

	Urban Heat Islands (°C)			
	Panel A: With Within-City Mobility Index			
	(1)	(2)	(3)	(4)
Within-city index	2.160***	0.986***	0.969***	1.494***
	(0.096)	(0.101)	(0.072)	(0.437)
Observations	27,453	27,453	27,453	27,453
R-square	0.355	0.700	0.806	0.467
	Panel B: With Move-In Index			
Move-in index	−0.709***	−0.304**	−0.132	1.549***
	(0.212)	(0.143)	(0.125)	(0.309)
Observations	27,701	27,701	27,701	27,701
R-square	0.301	0.699	0.805	0.483
	Panel C: With Move-Out Index			
Move-out index	−0.215***	0.103	0.050	1.062***
	(0.104)	(0.080)	(0.061)	(0.223)
Observations	27,701	27,701	27,701	27,701
R-square	0.301	0.699	0.805	0.479
City FEs	Y	Y		
DOW FEs	Y	Y	Y	
Month FEs		Y		
Year FEs		Y	Y	
City–month FEs			Y	
Day FEs				Y

DOW = day of week, FE = fixed effect.

Note: Standard errors in parentheses are clustered at the city level. *** = $p < 0.01$, ** = $p < 0.05$.

Source: Authors' calculations using surface urban heat island data from MODIS and mobility data from Baidu, described in Sections III.B and III.C respectively.

Table 2.1: Correlation of Urbanization Rate and Surface Urban Heat Island

	Urban Heat Islands (°C)	
	(1)	(2)
Urbanization rate	0.625*	0.311
	(0.349)	(1.705)
Urbanization rate^2		0.292
		(1.553)
Observations	223	223
R-square	0.014	0.014

Note: Urbanization rate ranges from 0.14 to 0.99.

Source: Authors' calculations using surface urban heat island data from MODIS and urbanization rate data from CEIC, described in Sections III.B and III.D respectively.

Table 3: Effects of COVID-19 Stringency on Surface Urban Heat Island

	Urban Heat Islands (°C)				
	(1)	(2)	(3)	(4)	(5)
Locked	0.148***	−0.096***	0.046	−0.094***	−0.102***
	(0.036)	(0.032)	(0.032)	(0.033)	(0.034)
LockedAnyCity	−0.033***	0.030*	0.022	0.041*	0.000
	(0.009)	(0.018)	(0.017)	(0.024)	(.)
Observations	455,345	455,345	455,345	455,345	455,345
R-square	0.000	0.249	0.324	0.249	0.256
Y-mean	−0.218	−0.218	−0.218	−0.218	−0.218
Y-sd	2.206	2.206	2.206	2.206	2.206
City FEs		Y		Y	Y
DOW FEs		Y	Y	Y	
Month FEs		Y			
Year FEs		Y	Y		
City–month FEs			Y		
Year–month FEs				Y	
Day FEs					Y

COVID-19 = coronavirus disease, DOW = day of week, FE = fixed effect.

Note: Estimates on LockedAnyCity, the single time term, are absorbed by day fixed effects in column (5). Standard errors in parentheses are clustered at the city level. *** = p < 0.01, * = p < 0.1.

Source: Authors' calculations using surface urban heat island data from MODIS, described in Section III.B.

Table 4: Heterogeneity Across Stringency Levels

	Urban Heat Islands (°C)			
	(1)	(2)	(3)	(4)
Locked1	−0.147***	0.127**	−0.142**	−0.146**
	(0.056)	(0.058)	(0.057)	(0.057)
Locked2	−0.101	−0.051	−0.111	−0.130
	(0.126)	(0.128)	(0.127)	(0.127)
Locked3	−0.067*	0.030	−0.069*	−0.076*
	(0.040)	(0.040)	(0.041)	(0.042)
LockedAnyCity1	0.026	0.011	0.053*	0.000
	(0.020)	(0.019)	(0.028)	(.)
LockedAnyCity2	.0558***	.0503**	.0623**	0.000
	(.0206)	(.0196)	(.0292)	(.)
LockedAnyCity3	-.00615	-.0031	-.00031	0.000
	(.024)	(.0229)	(.0299)	(.)
Observations	455,345	455,345	455,345	455,345
R-square	0.249	0.324	0.249	0.256
Y-mean	−0.218	−0.218	−0.218	−0.218
Y-sd	2.206	2.206	2.206	2.206
City FEs	Y		Y	Y
DOW FEs	Y	Y	Y	
Month FEs	Y			
Year FEs	Y	Y		
City–month FEs		Y		
Year–month FEs			Y	
Day FEs				Y

DOW = day of week, FE = fixed effect.

Note: Estimates on LockedAnyCity1-LockedAnyCity3, the single time terms, are absorbed by day fixed effects in column (4). Standard errors in parentheses are clustered at the city level. *** = p < 0.01, ** = p < 0.05, * = p < 0.1.

Source: Authors' calculations using surface urban heat island data from MODIS, described in Section III.B.

Table 5: Spillover Effects

	Urban Heat Islands (°C)			
	(1)	(2)	(3)	(4)
LockedAnyCity	0.030	0.018	0.040	0.000
	(0.018)	(0.017)	(0.024)	(.)
Locked	−0.095***	0.052	−0.099***	−0.110***
	(0.032)	(0.032)	(0.034)	(0.035)
LockedAnyCity×Adjacent	−0.038	0.041	−0.044	−0.051*
	(0.025)	(0.026)	(0.027)	(0.028)
LAC×NonAdj×SameProv	0.092***	0.028	0.082**	0.076**
	(0.034)	(0.034)	(0.035)	(0.035)
Observations	455,345	455,345	455,345	455,345
R-square	0.249	0.324	0.249	0.256
Y-mean	−0.218	−0.218	−0.218	−0.218
Y-sd	2.206	2.206	2.206	2.206
City FEs	Y		Y	Y
DOW FEs	Y	Y	Y	
Month FEs	Y			
Year FEs	Y	Y		
City–month FEs		Y		
Year–month FEs			Y	
Day FEs				Y

DOW = day of week, FE = fixed effect.

Note: Standard errors in parentheses are clustered at the city level. Estimates on LockedAnyCity, the single time term, are absorbed by day fixed effects in column (4). *** = p < 0.01, ** = p < 0.05, * = p < 0.1.

Source: Authors' calculations using surface urban heat island data from MODIS, described in Section III.B.

Table 6: Interacting with Time Trend

	Urban Heat Islands (°C)			
	(1)	(2)	(3)	(4)
Locked	−0.941***	−0.772**	−1.041***	−1.156***
	(0.314)	(0.317)	(0.327)	(0.329)
Locked×Days (×0.01)	0.102***	0.099***	0.114***	0.126***
	(0.038)	(0.038)	(0.039)	(0.039)
LockedAnyCity	0.028	0.020	0.036	0.000
	(0.018)	(0.017)	(0.025)	(.)
Days (×0.01)	0.049	0.036	0.056*	0.000
	(0.032)	(0.031)	(0.032)	(.)
Observations	455,345	455,345	455,345	455,345
R-square	0.249	0.324	0.249	0.256
Y-mean	−0.218	−0.218	−0.218	−0.218
Y-sd	2.206	2.206	2.206	2.206
City FEs	Y		Y	Y
DOW FEs	Y	Y	Y	
Month FEs	Y			
Year FEs	Y	Y		
City–month FEs		Y		
Year–month FEs			Y	
Day FEs				Y

DOW = day of week, FE = fixed effect.

Note: Standard errors in parentheses are clustered at the city level. *** = p < 0.01, ** = p < 0.05, * = p < 0.1.

Source: Authors' calculations using surface urban heat island data from MODIS, described in Section III.B.

Table 7: Interacting with Months

	Urban Heat Islands (°C)			
	(1)	(2)	(3)	(4)
Locked×Jan	−0.080	0.153	−0.082	−0.206
	(0.229)	(0.224)	(0.231)	(0.234)
Locked×Feb	−0.118**	0.028	−0.147***	−0.166***
	(0.048)	(0.048)	(0.053)	(0.054)
Locked×Mar	−0.197***	−0.077	−0.178***	−0.184***
	(0.060)	(0.061)	(0.063)	(0.065)
Locked×Apr	0.040	0.200	0.048	0.049
	(0.120)	(0.127)	(0.122)	(0.122)
Locked×May	-.376	-.225	-.377	-.405
	(.255)	(.256)	(.255)	(.255)
Locked×Jun	-.115	-.229	-.109	-.0896
	(.363)	(.361)	(.363)	(.363)
Locked×Jul	.0329	-.0573	.0726	.0903
	(.18)	(.176)	(.181)	(.183)
Locked×Aug	.106	.434***	.143	.145
	(.0888)	(.0931)	(.0909)	(.0907)
Locked×Sep	−2.45***	−2.58***	−2.48***	−2.4***
	(.439)	(.421)	(.44)	(.447)
Locked×Oct	.185	.256	.166	.128
	(.429)	(.423)	(.429)	(.429)
Locked×Nov	.195	.368	.189	.177
	(.267)	(.266)	(.267)	(.267)
Locked×Dec	.233	.176	.185	.189
	(.184)	(.184)	(.184)	(.184)
LockedAnyCity	.031*	.0227	.0465*	0.000
	(0.0179)	(.0171)	(.0245)	(.)
Observations	455,345	455,345	455,345	455,345
R-square	0.249	0.324	0.249	0.256
Y-mean	−0.218	−0.218	−0.218	−0.218
Y-sd	2.206	2.206	2.206	2.206
City FEs	Y		Y	Y
DOW FEs	Y	Y	Y	
Month FEs	Y			
Year FEs	Y	Y		
City–month FEs		Y		
Year–month FEs			Y	
Day FEs				Y

DOW = day of week, FE = fixed effect.

Note: Standard errors in parentheses are clustered at the city level. *** = p < 0.01, ** = p < 0.05, * = p < 0.1.

Source: Authors' calculations using surface urban heat island data from MODIS, described in Section III.B.

Table 8: Effects of COVID-19 Stringency on Human Mobility

	Panel A: Within-City Mobility Index			
	(1)	(2)	(3)	(4)
Locked	−0.387***	−0.428***	−0.387***	−0.268***
	(0.058)	(0.056)	(0.058)	(0.055)
LockedAnyCity	−1.871***	−1.869***	−1.871***	
	(0.051)	(0.050)	(0.051)	
Observations	36900	36900	36900	36900
R-square	0.752	0.818	0.752	0.841
Y-mean	4.108	4.108	4.108	4.108
	Panel B: Move-In Index			
Locked	−0.354***	−0.216***	−0.354***	−0.334***
	(0.065)	(0.039)	(0.065)	(0.067)
LockedAnyCity	−0.504***	−0.509***	−0.504***	
	(0.033)	(0.034)	(0.033)	
Observations	37,200	37,200	37,200	37,200
R-square	0.799	0.880	0.799	0.827
Y-mean	0.820	0.820	0.820	0.820
	Panel C: Move-Out Index			
Locked	−0.548***	−0.167***	−0.548***	−0.540***
	(0.126)	(0.041)	(0.126)	(0.133)
LockedAnyCity	−0.515***	−0.530***	−0.515***	
	(0.070)	(0.073)	(0.070)	
Observations	37,200	37,200	37,200	37,200
R-square	0.575	0.793	0.575	0.595
Y-mean	0.822	0.822	0.822	0.822
City FEs	Y		Y	Y
DOW FEs	Y	Y	Y	
Month FEs	Y			
Year FEs	Y	Y		
City–month FEs		Y		
Year–month FEs			Y	
Day FEs				Y

COVID-19 = coronavirus disease, DOW = day of week, FE = fixed effect.

Note: Estimates on LockedAnyCity, the single time term, are absorbed by day fixed effects in column (4). Standard errors in parentheses are clustered at the city level. *** = p < 0.01.

Source: Authors' calculations using mobility data from Baidu, described in Section III.C.

Table 9: Placebo Test

	Urban Heat Islands (°C)			
	(1)	(2)	(3)	(4)
Locked	0.083	0.139***	0.069	0.054
	(0.054)	(0.034)	(0.059)	(0.060)
LockedAnyCity	−0.034**	−0.038***	0.024	0.000
	(0.014)	(0.014)	(0.024)	(.)
Observations	364,152	364,152	364,152	364,152
R-square	0.249	0.326	0.249	0.255
Y-mean	−0.214	−0.214	−0.214	−0.214
Y-sd	2.203	2.203	2.203	2.203
City FEs	Y		Y	Y
DOW FEs	Y	Y	Y	
Month FEs	Y			
Year FEs	Y	Y		
City–month FEs		Y		
Year–month FEs			Y	
Day FEs				Y

DOW = day of week, FE = fixed effect.

Note: Standard errors in parentheses are clustered at the city level. *** = p < 0.01, ** = p < 0.05.

Source: Authors' calculations using surface urban heat island data from MODIS, described in Section III.B.

Table 10: Adding Group-Specific Time Trends

	Urban Heat Islands (°C)			
	(1)	(2)	(3)	(4)
Locked	−0.124***	0.020	−0.124***	−0.134***
	(0.032)	(0.033)	(0.033)	(0.034)
LockedAnyCity	0.029	0.022	0.037	0.000
	(0.018)	(0.017)	(0.025)	(.)
Observations	455,345	455,345	455,345	455,345
R-square	0.249	0.324	0.249	0.256
Y-mean	−0.218	−0.218	−0.218	−0.218
Y-sd	2.206	2.206	2.206	2.206
City FEs	Y		Y	Y
DOW FEs	Y	Y	Y	
Month FEs	Y			
Year FEs	Y	Y		
City–month FEs		Y		
Year–month FEs			Y	
Day FEs				Y

DOW = day of week, FE = fixed effect.

Note: Standard errors in parentheses are clustered at the city level. *** = p < 0.01.

Source: Authors' calculations using surface urban heat island data from MODIS, described in Section III.B.

Table 11: Using Lunar Calendar

	Urban Heat Islands (°C)			
	(1)	(2)	(3)	(4)
Locked	−0.086***	0.028	−0.110***	−0.102***
	(0.032)	(0.032)	(0.033)	(0.034)
LockedAnyCity	−0.022	−0.034*	−0.033	0.000
	(0.021)	(0.020)	(0.027)	(.)
Observations	453,832	453,832	453,832	453,832
R-square	0.249	0.321	0.249	0.256
Y-mean	−0.218	−0.218	−0.218	−0.218
Y-sd	2.206	2.206	2.206	2.206
City FEs	Y		Y	Y
DOW FEs	Y	Y	Y	
Month FEs	Y			
Year FEs	Y	Y		
City–month FEs		Y		
Year–month FEs			Y	
Day FEs				Y

DOW = day of week, FE = fixed effect.

Note: Standard errors in parentheses are clustered at the city level. *** = p < 0.01, * = p < 0.1.

Source: Authors' calculations using surface urban heat island data from MODIS, described in Section III.B.

Table 12: Effects on Nighttime Heat Island

	Urban Heat Islands (°C)			
	(1)	(2)	(3)	(4)
Locked	−0.053***	−0.001	−0.068**	−0.078***
	(0.026)	(0.027)	(0.028)	(0.028)
LockedAnyCity	0.058***	0.054***	0.064***	0.000
	(0.015)	(0.015)	(0.021)	(.)
Observations	452,087	452,087	452,087	452,087
R-square	0.242	0.297	0.242	0.248
Y-mean	−0.005	−0.005	−0.005	−0.005
Y-sd	1.896	1.896	1.896	1.896
City FEs	Y		Y	Y
DOW FEs	Y	Y	Y	
Month FEs	Y			
Year FEs	Y	Y		
City–month FEs		Y		
Year–month FEs			Y	
Day FEs				Y

DOW = day of week, FE = fixed effect.

Note: Standard errors in parentheses are clustered at the city level. *** = p < 0.01, ** = p < 0.05.

Source: Authors' calculations using surface urban heat island data from MODIS, described in Section III.B.

REFERENCES

ADB. 2021. *Disaster Resilience in Asia—a Special Supplement of Asia's Journey to Prosperity: Policy, Market, and Technology Over 50 Years*. Manila: Asian Development Bank.

Agarwal, Sumit, Keyang Li, Yu Qin, Jing Wu, and Jubo Yan. 2020. "Household Asset Portfolios During the COVID-19 Pandemic." http://dx.doi.org/10.2139/ssrn.3674702.

Alqasemi, Abduldaem S., Mohamed E. Hereher, Gordana Kaplan, Ayad M. Fadhil Al-Quraishi, and Hakim Saibi. 2021. "Impact of COVID-19 Lockdown Upon the Air Quality and Surface Urban Heat Island Intensity over the United Arab Emirates." *Science of The Total Environment* 767: 144330. doi: https://doi.org/10.1016/j.scitotenv.2020.144330.

Angrist, Joshua D., and Jörn-Steffen Pischke. 2009. *Mostly Harmless Econometrics: An Empiricist's Companion*. Princeton, NJ: Princeton University Press.

Bavel, Jay J. Van, Katherine Baicker, Paulo S. Boggio, Valerio Capraro, Aleksandra Cichocka, Mina Cikara, Molly J. Crockett, Alia J. Crum, Karen M. Douglas, James N. Druckman, John Drury, Oeindrila Dube, Naomi Ellemers, Eli J. Finkel, James H. Fowler, Michele Gelfand, Shihui Han, S. Alexander Haslam, Jolanda Jetten, Shinobu Kitayama, Dean Mobbs, Lucy E. Napper, Dominic J. Packer, Gordon Pennycook, Ellen Peters, Richard E. Petty, David G. Rand, Stephen D. Reicher, Simone Schnall, Azim Shariff, Linda J. Skitka, Sandra Susan Smith, Cass R. Sunstein, Nassim Tabri, Joshua A. Tucker, Sander van der Linden, Paul van Lange, Kim A. Weeden, Michael J. A. Wohl, Jamil Zaki, Sean R. Zion, and Robb Willer. 2020. "Using Social and Behavioural Science to Support COVID-19 Pandemic Response." *Nature Human Behaviour* 4 (5): 460–71. doi: 10.1038/s41562-020-0884-z.

Beyer, Robert C. M., Tarun Jain, and Sonalika Sinha. 2020 "Lights Out? COVID-19 Containment Policies and Economic Activity". Policy Research Working Paper 9485. World Bank. Washington, DC.

Carnahan, Walter H., and Robert C. Larson. 1990. "An Analysis of an Urban Heat Sink." *Remote Sensing of Environment* 33 (1): 65–71. doi: https://doi.org/10.1016/0034-4257(90)90056-R.

Chen, Haiqiang, Wenlan Qian, and Qiang Wen. 2021. "The Impact of the COVID-19 Pandemic on Consumption: Learning from High-Frequency Transaction Data." *AEA Papers and Proceedings* 111: 307–11. doi: 10.1257/pandp.20211003.

Chen, Joy, Zijun Cheng, Kaiji Gong, and Jinlin Li. 2020. "Riding out the COVID-19 Storm: How Government Policies Affect SMEs in China." http://dx.doi.org/10.2139/ssrn.3660232.

Chen, Zhuo, Pengfei Li, Li Liao, and Zhengwei Wang. 2020. "Assessing and Addressing the Coronavirus-Induced Economic Crisis: Evidence from 1.5 Billion Sales Invoices." PBCSF-NIFR Research Paper. Tsinghua University. Beijing. http://dx.doi.org/10.2139/ssrn.3661014.

Dong, Mengchen, Giuliana Spadaro, Shuai Yuan, Yue Song, Zi Ye, and Xin Ren. 2021. "Self-Interest Bias in the COVID-19 Pandemic: A Cross-Cultural Comparison between the United States and China." *Journal of Cross-Cultural Psychology* 52 (7): 663–79. doi: 10.1177/00220221211025739.

Fang, Hanming, Long Wang, and Yang Yang. 2020. "Human Mobility Restrictions and the Spread of the Novel Coronavirus (2019-nCov) in China." *Journal of Public Economics* 191: 104272. doi: https://doi.org/10.1016/j.jpubeco.2020.104272.

Gelfand, Michele J., Jesse R. Harrington, and Joshua Conrad Jackson. 2017. "The Strength of Social Norms across Human Groups." *Perspectives on Psychological Science* 12 (5): 800–09. doi: 10.1177/1745691617708631.

Gunay, Samet, Gökberk Can, and Murat Ocak. 2020. "Forecast of China's Economic Growth During the COVID-19 Pandemic: A MIDAS Regression Analysis." *Journal of Chinese Economic and Foreign Trade Studies* 14(1): 3–17.

Havrlant, David, Abdulelah Darandary, and Abdelrahman Muhsen. 2021. "Early Estimates of the Impact of the COVID-19 Pandemic on GDP: A Case Study of Saudi Arabia." *Applied Economics* 53 (12): 1317–25. doi: 10.1080/00036846.2020.1828809.

Kim, Beomsoo, and Yang Zhao. 2020. "Psychological Suffering Owing to Lockdown or Fear of Infection? Evidence from the COVID-19 Outbreak in China." Discussion Paper Series. Institute of Economic Research, Korea University. Seoul.

Li, Xiaoma, and Weiqi Zhou. 2019. "Spatial Patterns and Driving Factors of Surface Urban Heat Island Intensity: A Comparative Study for Two Agriculture-Dominated Regions in China and the USA." *Sustainable Cities and Society* 48: 101518. doi: https://doi.org/10.1016/j.scs.2019.101518.

Li, Xiaoma, Yuyu Zhou, Ghassem R. Asrar, Marc Imhoff, and Xuecao Li. 2017. "The Surface Urban Heat Island Response to Urban Expansion: A Panel Analysis for the Conterminous United States." *Science of The Total Environment* 60506: 426–35. doi: https://doi.org/10.1016/j.scitotenv.2017.06.229.

Li, Xuecao, Peng Gong, Yuyu Zhou, Jie Wang, Yuqi Bai, Bin Chen, Tengyun Hu, Yixiong Xiao, Bing Xu, Jun Yang, Xiaoping Liu, Wenjia Cai, Huabing Huang, Tinghai Wu, Xi Wang, Peng Lin, Xun Li, Jin Chen, Chunyang He, Xia Li, Le Yu, Nicholas Clinton, and Zhiliang Zhu. 2020. "Mapping Global Urban Boundaries from the Global Artificial Impervious Area (GAIA) Data." *Environmental Research Letters* 15 (9): 094044. doi: 10.1088/1748-9326/ab9be3.

Lin, Zhixian, and Christopher M. Meissner. 2020. "Health Vs. Wealth? Public Health Policies and the Economy During COVID-19." NBER Working Paper Series No. 27099. National Bureau of Economic Research. Cambridge, MA. 10.3386/w27099.

Miguel, Edward, and Michael Kremer. 2004. "Worms: Identifying Impacts on Education and Health in the Presence of Treatment Externalities". *Econometrica* 72 (1): 159217. doi: https://doi.org/10.1111/j.1468-0262.2004.00481.x

Miguel, Edward and A. Mushfiq Mobarak. 2021. "The Economics of the COVID-19 Pandemic in Poor Countries." *Annual Review of Economics*, forthcoming.

Min, Shi, Cheng Xiang, and Xiao-heng Zhang. 2020. "Impacts of the COVID-19 Pandemic on Consumers' Food Safety Knowledge and Behavior in China." *Journal of Integrative Agriculture* 19 (12): 2926–36. doi: https://doi.org/10.1016/S2095-3119(20)63388-3.

Niu, Lu, Ronglin Tang, Yazhen Jiang, and Xiaoming Zhou. 2020. "Spatiotemporal Patterns and Drivers of the Surface Urban Heat Island in 36 Major Cities in China: A Comparison of Two Different Methods for Delineating Rural Areas." *Sustainability* 12 (2). doi: 10.3390/su12020478.

Peroff, Kathleen, and Margaret Podolak-Warren. 1979. "Does Spending on Defence Cut Spending on Health?: A Time-Series Analysis of the U.S. Economy 1929–74." *British Journal of Political Science* 9 (1): 21–39. doi: 10.1017/S0007123400001605.

Ruan, Jianqing, Qingwen Cai, and Songqing Jin. 2021. "Impact of COVID-19 and Nationwide Lockdowns on Vegetable Prices: Evidence from Wholesale Markets in China." *American Journal of Agricultural Economics* 103 (5): 1574-94. doi: https://doi.org/10.1111/ajae.12211.

Shimul, Shafiun Nahin, Angi Alradie-Mohamed, Russell Kabir, Abdulrahman Al-Mohaimeed, and Ilias Mahmud. 2021. "Effect of Easing Lockdown and Restriction Measures on COVID-19 Epidemic Projection: A Case Study of Saudi Arabia." *PLOS ONE* 16(9): e0256958. doi: 10.1371/journal.pone.0256958.

Wang, Shenmin, Qifang Ma, Haiyong Ding, and Hanwei Liang. 2018. "Detection of Urban Expansion and Land Surface Temperature Change Using Multi-Temporal Landsat Images." *Resources Conservation and Recycling* 128: 526–34. doi: 10.1016/j.resconrec.2016.05.011.

Zhang, Linlin, Qingyan Meng, Zhenhui Sun, and Yunxiao Sun. 2017. "Spatial and Temporal Analysis of the Mitigating Effects of Industrial Relocation on the Surface Urban Heat Island over China." *ISPRS International Journal of Geo-Information* 6 (4). doi: 10.3390/ijgi6040121.

Zhang, Xiaoming, Weijie Luo, and Jingci Zhu. 2021. "Top-Down and Bottom-up Lockdown: Evidence from COVID-19 Prevention and Control in China." *Journal of Chinese Political Science* 26 (1): 189–211. doi: 10.1007/s11366-020-09711-6.

Zhou, Bin, Diego Rybski, and Jürgen P. Kropp. 2017. "The Role of City Size and Urban Form in the Surface Urban Heat Island." *Scientific Reports* 7 (1): 4791. doi: 10.1038/s41598-017-04242-2.

Zhou, Decheng, Jingfeng Xiao, Stefania Bonafoni, Christian Berger, Kaveh Deilami, Yuyu Zhou, Steve Frolking, Rui Yao, Zhi Qiao, and José A. Sobrino. 2019. "Satellite Remote Sensing of Surface Urban Heat Islands: Progress, Challenges, and Perspectives." *Remote Sensing* 11 (1). doi: 10.3390/rs11010048.

Zhou, Decheng, Shuqing Zhao, Shuguang Liu, Liangxia Zhang, and Chao Zhu. 2014. "Surface Urban Heat Island in China's 32 Major Cities: Spatial Patterns and Drivers." *Remote Sensing of Environment* 152: 51–61. doi: https://doi.org/10.1016/j.rse.2014.05.017.

Zhou, Decheng, Shuqing Zhao, Liangxia Zhang, Ge Sun, and Yongqiang Liu. 2015. "The Footprint of Urban Heat Island Effect in China." *Scientific Reports* 5: 11160–60. doi: 10.1038/srep11160.

Economic Impact of COVID-19 Containment Policies

Evidence Based on Novel Surface Heat Data from the People's Republic of China

Governments have adopted various policies and measures to control the spread of coronavirus disease (COVID-19) pandemic. This paper uses novel high-frequency and spatially granular surface urban heat island (SUHI) data from satellites to quantify the impact of pandemic-related containment policies on economic output in the People's Republic of China. Results suggest containment measures decreased SUHI in locked cities marginally; generated positive and negative spillover effects in unlocked cities, with positive effects dominating; and initial experiences helped inform management of these measures.

About the Asian Development Bank

ADB is committed to achieving a prosperous, inclusive, resilient, and sustainable Asia and the Pacific, while sustaining its efforts to eradicate extreme poverty. Established in 1966, it is owned by 68 members —49 from the region. Its main instruments for helping its developing member countries are policy dialogue, loans, equity investments, guarantees, grants, and technical assistance.

ADB

ASIAN DEVELOPMENT BANK
6 ADB Avenue, Mandaluyong City
1550 Metro Manila, Philippines
www.adb.org